Heterogeneity effects in soil water transferences process under unsaturated conditions in alluvial soil in the mesoscale

Peronico, R. L.; Rabelo, A. E. C. G. C.; Coutinho, A. P.; Santos Neto, S. M.; Melo, T. A. T.; Silva Neto, J. A.; Alves, E. M; Antonino, A. C. D.

Abstract

This paper presents a hydrodynamic modeling of the unsaturated zone with a heterogeneous profile in an alluvial soil in the Capibaribe River Basin. Three-dimensional infiltration tests were carried out with the aim to do the hydrodynamic characterization applying Beerkan Methodology through the BEST algorithm. Therefore, were used single ring infiltrometers. The soil profile was characterized with the Ground Penetrating Radar (GPR). The water transfer processes were simulated with the Hydrus Modell. The simulations demonstrated that the heterogeneity of the soil generated preferential flows. In a heterogeneous soil profile was observed the presence of a capillary barrier phenomenon, generating impact on the spatial variability of water storage on the soil profile.

Keywords: *Subsurface modeling, preferential flow.*

1. Introduction

Studies on soil water transfer are relevant for interpreting and modeling hydrological processes in the unsaturated zone (UZ), principally to determine the hydraulic properties of the soil in field scale. These properties are represented by hydrodynamic parameters, such as retention curve in general (Alagna et al., 2016, Antonino et al., 2001; Lèger et al., 2013). The UZ is very important for understanding the water cycle of a region, as it mediates the partition of the volume that reaches the surface and the part transferred to the aquifers. Moreover, the vadose zone acts as a reservoir of water and/or chemical substances, where it assists in the control of soil contamination (Winiarski et al., 2013).

These studies become more relevant when the regions are in areas of great water shortage. The communities of these regions use groundwater, water-trunk and rainfall water as the main source of water supply (Xi, et al., 2016). The Brazilian semi-arid region presents a lower precipitation rate, generating water availability difficulty for economic activities and human supply. Thus, alluvial deposits, characterized by small depth reservoir, have fundamental importance for water supply in the semi-arid regions of the Brazilian northeast (Ribeiro Filho et al., 2017; Cirilo et al., 2016). Therefore, characterizing alluvial aquifers is the key for a sustainable management of the scarce water resources in this region. The

hypothesis that the soil is homogeneous in field scale is adopted to quantify the storage and recharge capacity of these aquifers. This context neglects the impacts that a heterogeneous profile can cause in the vadose zone flow processes (Coutinho et al., 2015). This can lead to estimation errors, which put the water resources at risk. This paper presents a hydrodynamic modeling of the unsaturated zone with a heterogeneous profile in an alluvial soil in the Capibaribe River Basin in the state of Pernambuco, Brazil.

2. Methodology

2.1. Experimentation site

This study was performed in the Poço da Lama Grange located on the border between the cities of Brejo da Madre de Deus and Santa Cruz do Capibaribe. The geographic localization is 7º56'57.6"S and 36º17'57.2"W in the Capibaribe dry riverbed, Figure 1. Both cities are situated in the west mesoregion of Ipojuca Valley microregion. This City belongs to Capibaribe River hydrographic basin and is inserted in a hydrogeological fissure domain. This domain consists of a rocks crystal basement composed of metamorphic, igneous, and calcium-alkaline rocks.

Figure 1 - Santa Cruz do Capibaribe and Brejo da Madre de Deus localization.

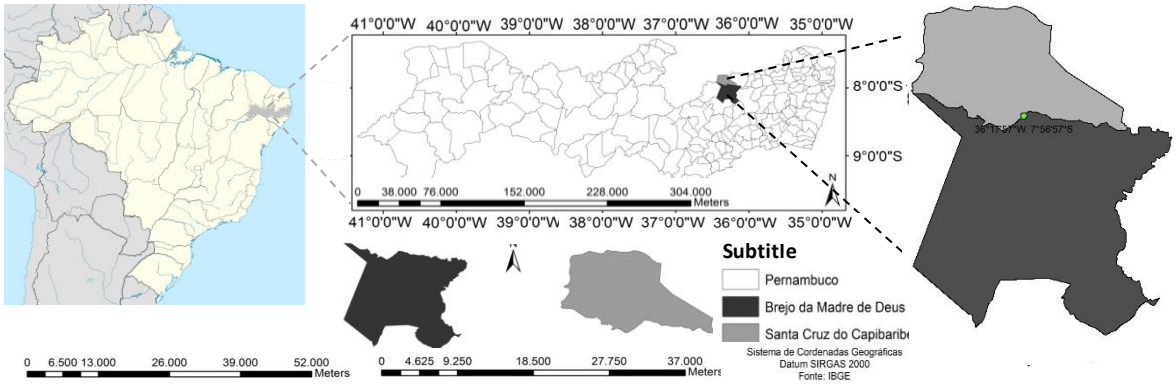

The Capibaribe river springs on the border of the cities Jataúba and Porção, covering an extension of 280 km until Recife, where it reaches the Atlantic Ocean (CPRM, 2005). The Capibaribe River has a high economic importance in Pernambuco State, because of its use on agricultural, livestock, Industry and residential activities. (Araújo Filho, 2014). This region has moderated dry climate based on the INMET classification. The precipitation volume is low and in 2016 the maximum monthly rainfall volume measured was 82.5 mm/month in January. The precipitation history of Brejo da Madre de Deus and Santa Cruz do Capibaribe are demonstrated in Figure 2. The native vegetal cover is Caatinga (Braga et al., 2016).

Figure 2 - Precipitation data for Santa Cruz do Capibaribe (S.C.C.) and Brejo da Madre de Deus (B.M.D.).

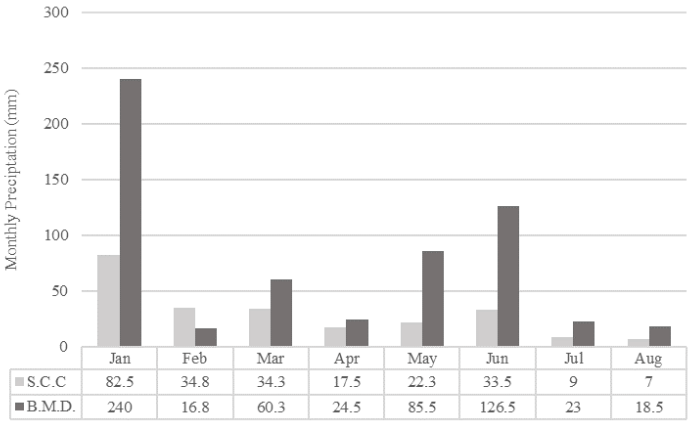

	Jan	Feb	Mar	Apr	May	Jun	Jul	Aug
S.C.C	82.5	34.8	34.3	17.5	22.3	33.5	9	7
B.M.D.	240	16.8	60.3	24.5	85.5	126.5	23	18.5

The soil at the study field was characterized as alluvium and has layers of different textural classes (EMBRAPA, 2000). A trench was opened with 10m length, 3m depth and 2m width. In Figure 3a can be seen four kinds of soil textural classes: Loamy sand, sand, coarse sand and fine gravel.

The superficial layer was characterized as loamy sand, presenting organic matter and fine particles, which were deposited in floods periods, Figure 3b. The sandy characteristic favors the utilization of the GPR.

Figure 3 - Trench of soil profile. a) Profile trench, b) Soil profile.

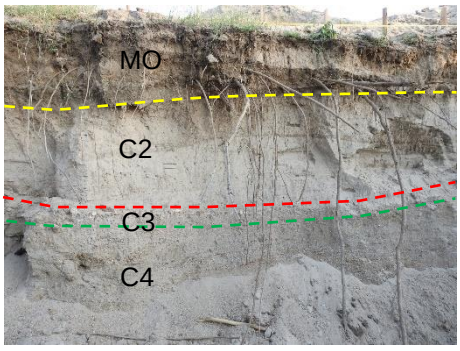

(a) Profile trench. (b) Soil profile.

M.O. – Superficial Layer (Loamy sand); C2 – Second Layer (Sand); C3 – Third Layer (Fine Gravel); C4 – Fourth Layer (Coarse Sand).

2.2. Soil hydrodynamic characterization - Beerkan Method and BEST algorithmic

The characterization of the soil hydraulic properties was achieved using BEST (Beerkan Estimation of Soil Transfer parameters) method. BEST was first presented by Lassabatère et al. (2006) and has the advantage of providing a complete characterization of both soil water retention and hydraulic conductivity functions.

BEST is based on the use of the van Genuchten (1980) relationship for the water retention curve with the Burdine (1953) condition and the Brooks and Corey (1964) relationship for hydraulic conductivity, since they were found to be accurate for describing the hydraulic behavior of most soil types (Fuentes *et al.*, 1992):

$$\frac{\theta-\theta_r}{\theta_s-\theta_r}=\left[1+\left(\frac{h}{h_g}\right)^n\right]^{-m} \quad [1a]$$

$$m=1-\frac{k_m}{n} \quad [1b]$$

$$\frac{K(\theta)}{K_s}=\left(\frac{\theta-\theta_r}{\theta_s-\theta_r}\right)^{\eta} \quad [2a]$$

$$\eta=\frac{2}{m\times n}+2+p \quad [2b]$$

where θ (L^3L^{-3}) is the volumetric soil water content, h (L) is the water pressure head, K ($L\ T^{-1}$) is the soil hydraulic conductivity, n, m and η are shape parameters, k_m is a user index (Haverkamp *et al.*, 2006; Di Prima et al., 2016), p is a tortuosity parameter, and h_g (L), representing the inflection point of the water retention curve, θ_S (L^3L^{-3}, field-saturated soil water content), θ_r (L^3L^{-3}, residual soil water content) and K_S ($L\ T^{-1}$, field-saturated soil hydraulic conductivity) are scale parameters.

In order to estimate all hydraulic parameters, BEST methods require two sets of data: i) particle-size distribution (PSD) of the soil and bulk density, and ii) cumulative infiltration along with the initial and final soil water contents of the infiltration experiment. In BEST, θ_r is assumed to be zero. The saturated water content θ_S is derived from the value of bulk density assuming it equals porosity. For shape parameters, BEST considers Burdine's model (1953) leading to m=1-2/n (k_m = 2) and η = 2/(mn)+3 (p=1).

The estimation of the shape parameters by BEST uses the approach proposed by Haverkamp et al. (2006). These authors consider that, for an infiltration experiment with zero water pressure on a circular surface of radius, r (L), above a uniform soil with a uniform water content, θ_i, the three-dimensional cumulative infiltration, I (L), and the infiltration rate, i ($L\ T^{-1}$), can be described by the following explicit transient, Eqs.[3a] and [3b] and steady-state, Eqs.[3c] and [3d] expressions (Haverkamp *et al.*, 1994; Aiello et al., 2014):

$$I(t)=S\sqrt{t}+\left(A\,S^2+B\,K_s\right)t \quad [3a]$$

$$i(t)=\frac{S}{2\sqrt{t}}+\left(A\,S^2+B\,K_s\right) \quad [3b]$$

$$I_{sst}(t)=\left(A\,S^2+K_s\right)t+C\frac{S^2}{K_s} \quad [3c]$$

$$i_{sst}(t)=A\,S^2+K_s \quad [3d]$$

where t (T) is the time and A (L^{-1}), B (-) and C (-) are constants that can be defined for the specific case of a Brooks and Corey (1964) relationship as:

$$A = \frac{\gamma}{r\left(\theta_s - \theta_i\right)} \quad [4a]$$

$$B = \frac{2-\beta}{3}\left[1-\left(\frac{\theta_i}{\theta_s}\right)^{\eta}\right]+\left(\frac{\theta_i}{\theta_s}\right)^{\eta} \quad [4b]$$

$$C = \frac{1}{2\left(1-\beta\right)\left[1-\left(\frac{\theta_i}{\theta_s}\right)^{\eta}\right]}\ln\left(\frac{1}{\beta}\right) \quad [4c]$$

where β and γ are coefficients that are commonly set at 0.6 and 0.75, respectively, for θ_i < 0.25 θ_s (Haverkamp *et al.*, 1994; Smettem *et al.*, 1994). More recent investigations suggested that the values of β and γ scarcely depend on the initial degree of saturation but can be soil dependent (Lassabatere *et al.*, 2009).

2.3. GPR Characterization

The ground penetrating radar (GPR) was used for the structural mapping of the soil profile to identify the different existing materials. For this purpose, an antenna of a frequency of 400MHz was used, applying the “offset mode” (Neal, 2004). The mapped profile had dimensions of 3 meters of depth and 10 meters of length.

For the calibration of the equipment, an iron rod was placed in a depth of one meter. The hyperboles generated by the images in this profile help to calibrate the distance and speed of the wave that was used. The average travel velocity of the electromagnetic wave for this profile was 0.11 ns.

Data were treated in the five steps: 1) distance normalization, 2) correct position, 3) migration, 4) background removal and 5) filters. Then, after these steps, the information collected was interpreted (Coutinho et al., 2015).

Irregularities on the field in thus the GPR to identify a small layer of air, which should be taken off during the treatment. This must be done with caution, so information is not lost (Goutaland et al., 2008).

In the migration treatment, the energy of the emitted signal is attenuated as the electromagnetic wave (EMW) travels to a deeper layer. Besides that, a shallow object will submit the EMW to the diffraction phenomenon. Then, the propagation energy is smaller than when it was generated. Thus, deeper objects can be overshadowed, leading to a misinterpretation of the image. Another utility of this treatment is the correction of geometry distortions and size of the underground buried objects images.

The background treatment allows the suppression of horizontal reflectors at a depth where the amplitude is constant.

The filters treatment is defined as the response of a pulse that can have finite or infinite duration. They are applied to the removal of low-frequency or high-frequency noises both in the horizontal and vertical directions. They can be of three type: "Infinite Impulse Response" (IIR), “Finite Impulse Response" (FIR) and "Spatial 2-D Filters ".

In the interpretation phase, it is necessary to observe the continuity of the structures that were identified in a section.

2.4. Hydrus Modelling

The HYDRUS 2D/3D software was utilized to simulate the water internal drainage in the profile solving the Richards equations, Eq [5]. For this propose the boundary conditions used were: a) absence of flow at the profile surface and sides; b) free drainage at the profile bottom. The free drainage of the profile means that the bottom flow is only dependent on the hydraulic conductivity, (i.e., the hydraulic gradient is unitary). The initial soil was considerate near to the saturation.

$$\frac{\partial\theta(h)}{\partial t} = \frac{\partial}{\partial z}\left[K_z(h)\cdot\nabla(h+z)\right] + \frac{\partial}{\partial x}\left[K_x(h)\cdot\nabla(h+x)\right] - S \qquad [5]$$

The importance of first assessing the moisture profile for the internal drainage is the possibility to observe the preferential flows without the influence of large potential rates on the surface. This shows the behavior of the soil can have due to the different existing materials. It was chosen a 30 days drainage period with the aim to have a stable soil, which would present a significant amount of water. Therefore, a 26-cm mesh was used with 720 knots, 240 1D elements and 1336 2D elements.

3. Results and Discursion

3.1. Infiltration Tests

The cumulative infiltration tests with single ring infiltrometers were performed three times for each layer. But these experiments were not done on the Fine Gravel layer, because of its thickness. Then, for the Fine Gravel, the Arya and Paris (1981) methodology was utilized. The shorter and longer infiltration test duration time were 399 and 9116 seconds, respectively. The infiltrated water and time are can be seen in Table 1. Even though the granulometric classification indicates sandy texture for all layers, it was observed the distinction behavior existing in the profile for the accumulated infiltration. These hydrodynamic differences are not only generated by the granulometry but also depends on the pores size distribution and the soil compaction.

Table 1 - Total infiltrated water (T.I.W.) and Time (s) for the infiltration tests.

	MO-R1	MO-R2	MO-R3	Average
T.I.W. (mm)	1094.35	340.466	1487.200	974.01
Time (s)	3807	7172	9112	6697.00
	C2-R1	C2-R2	C2-R3	
T.I.W. (mm)	1543.321	1431.079	841.811	1272.07
Time (s)	1627	711	931	1089.67
	C4-R1	C4-R2	C4-R3	
T.I.W. (mm)	785.691	1571.381	2329.011	1562.03
Time (s)	422	399	1432	751.00

R1 – First test; R2 – Second test; R3 – Third test.

The hydrodynamic properties are presented in Table 2. The direct adjustments of the cumulative infiltration curves were not made, because some parameters may have no physical sense. This is since the equations are developed for the homogeneous, isotropic and isothermal profile. The difference of layers in the profile can generate errors, where the values of the saturated hydraulic conductivity obtained in some cases can be negative (Lassabatère et al., 2006).

Vanderveare et al. (2000) proposed one way to see the influences in the cumulative infiltration curve, which was the linearization of infiltration tests, as showed in Eq. [6]. This linearization is presented in Figure 4. The slope of this curve expresses the influence of the hydraulic conductivity in relation to the accumulated infiltration, Equation [3a]. Then, its decrease indicates a reduction of the profile hydraulic conductivity to the existence of a hydraulic barrier between layers.

$$\begin{array}{rccc} f: & A & \rightarrow & B \\ & sqrt(t) & \mapsto & L.I. \end{array} \qquad [6]$$

were $L.I. = \dfrac{I(t)}{\sqrt{t}}$.

Table 2 – Soil hydrodynamic properties.

	θ_r ($cm^3.cm^{-3}$)	θ_s ($cm^3.cm^{-3}$)	α (1/cm)	n (-)	K_s ($cm.min^{-1}$)
MO	0.004	0.483	6.515	1.327	0.900
C2	0.010	0.534	4.410	1.437	1.115
C3	0.020	0.360	111.600	2.700	36.000
C4	0.004	0.470	2.410	1.682	1.104

M.O. – Superficial Layer (Loamy sand); C2 – Second Layer (Sand);
C3 – Third Layer (Fine Gravel); C4 – Fourth Layer (Coarse Sand).

Since the hydraulic conductivity of the soil is directly dependent on the existing water volume, the finer layer MO (loamy sand) has a high retention capacity.

This makes the conductivity of the next layer C2 (sand) dependent of the MO layer water supplied volume. Because of its low water volume, the C2 layer has small hydraulic conductivity. This leads the graph to a decrease in its slope.

Figure 4 - Linearization of the cumulative infiltration test.

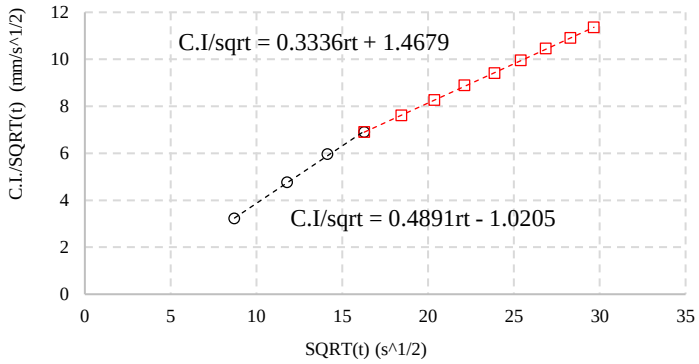

3.2. GPR data analyses

The radargram obtained with the application of a GPR antenna of 400MHz frequency is shown in Figure 5. It is observed the presence of long and horizontal reflectors during approximately the first sixty centimeters. This manifestation of the geophysical signal in the first unit reflects the influence of the soil surface layer, composed of a mixture of medium sand, organic matter and grass roots.

From fifty centimeters deep are observed regions of greater attenuation of the electromagnetic signal (between six and ten meters in the abscissa). These regions correspond to fine sand layers. Between fifty centimeters and a meter and a half of depth, it is possible to observe a series of small curved and discontinuous reflectors. These reflectors indicate the presence of a mixture of coarse sand and fine gravel.

Figure 5 - GPR profile with the 400MHz antenna.

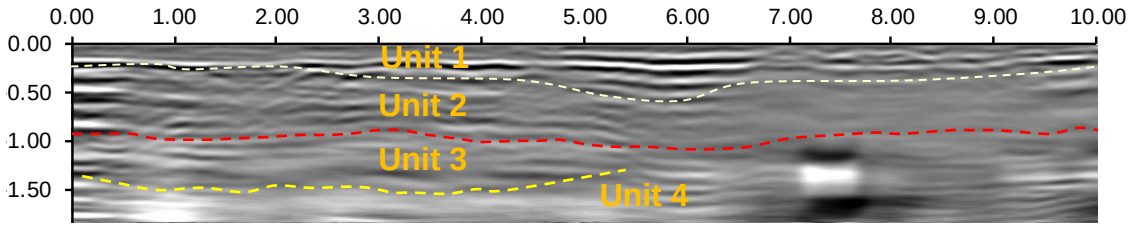

This geophysical characterization from a trench allows relating the heterogeneities to their respective geophysical signatures. This allows with the help of the GPR to increase the knowledge of the subsoil heterogeneities in a non-destructive way on a larger scale than that of excavation.

3.3. Hydrus Simulation

The map and graphics of 5 observation sections (3 vertical and 2 horizontal) of the initial moisture distribution of profile internal drainage simulation are demonstrated in Figure 6. It is observed that moisture distribution at the surface and at the base is constant. It is also noticed that for the three points of observation there is a marked drop for the existing gravel layer.

Figure 6 - Initial simulation profile for the internal drainage: a) Initial moisture profile, b) Initial top moisture, c) Initial bottom moisture, d) Initial 9m transection moisture, e) Initial 6m transection moisture, f) Initial 1m transection moisture.

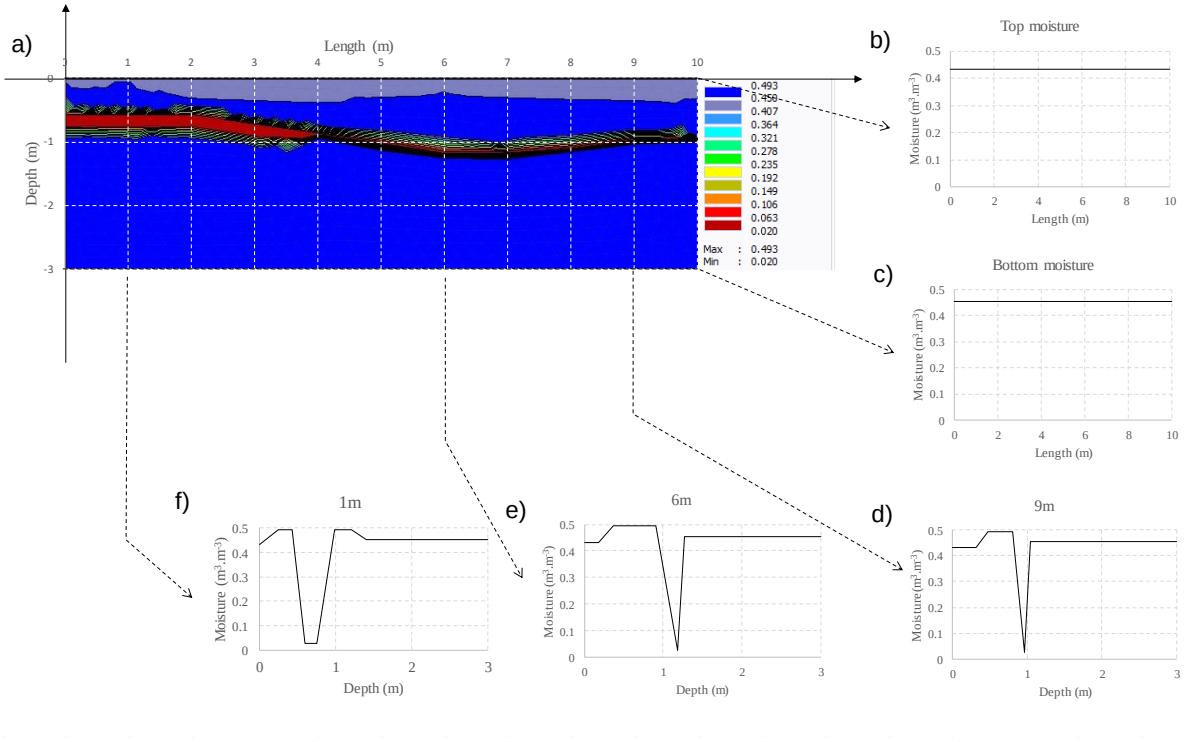

After the first four hours of testing the soil already showed a large water carrying capacity, where the surface and base humidity decreased around 30%, Figure 7. The moisture profiles for the three observation nodes show a reduction of the mean value of moisture, being more visible for the layers below the fine gravel soil. This is due to the fact that the gravel layer acts as a hydraulic barrier to water flow. So, despite presenting a high saturated hydraulic conductivity, in unsaturated conditions, its value is not large enough to allow high flow. Its capillary forces are very small when compared to the layer immediately above. Because of that, the transport of water to the gravel layer dependents on the volume of water provided by the preceding layer. This last one has a very low saturated conductivity when compared to the gravel. A high spatial variability of water storage is observed, which is an effect of the heterogeneity throughout a same horizontal (Coutinho et al., 2015; Prédélus et al., 2015).

Figure 7 - Drainage profile to the 4 hours simulation: a) Moisture profile, b) Top moisture, c) Bottom moisture, d) 9m transection moisture, e) 6m transection moisture, f) 1m transection moisture.

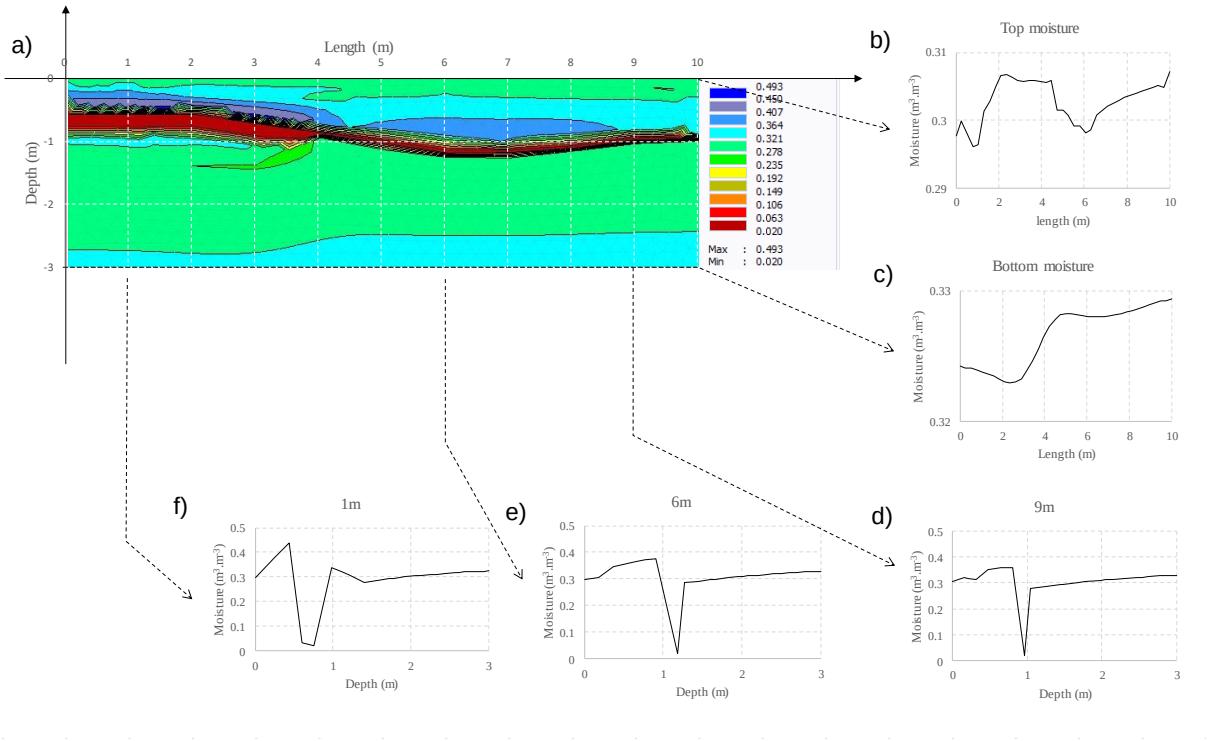

In the moisture distribution graphics of the top and bottom profile are observed the performance of the existing hydraulic barriers on the profile. These barriers are located at the interfaces between layers of different textures. Where it is shown that its effects are higher at the distances from 0 to 4 meters. This causes a larger accumulation of water at the top of the profile and a preferential flow on the fine gravel layer. However, between 2 and 4 meters of the profile horizontal distance, the graphs do not explicitly show this existence. Nevertheless, when looking at the profile isolines graph, it is shown the existence of a preferential flow due to the inclination that these materials are arranged.

This influence of the hydraulic barriers on the generation of the preferential flow is explicit when observing the velocity map of the profile, Figure 8. In the distance from 2 to 4 meters is observed the existence of a preferential flow for the times of 0h, 4h and 12 hours. This leads to a greater accumulation of water in this location, which is occasioned by the hydraulic barriers of the different textures layers.

Besides that, the greatest flow potential is observed for the gravel and coarse sandy layers. So, this influence is directly dependent on the hydraulic conductivity. Thus, it is generated a rapid stabilization of the drainage in the profile. Where for a drainage period of 30 days occurs a small variation in the profile. This providing a drainage of 910.2mm during this period.

Figure 8 - Velocity vector profile: a) Initial time velocity vector map, b) 4 hours velocity vector map, c) 12 hours velocity vector map.

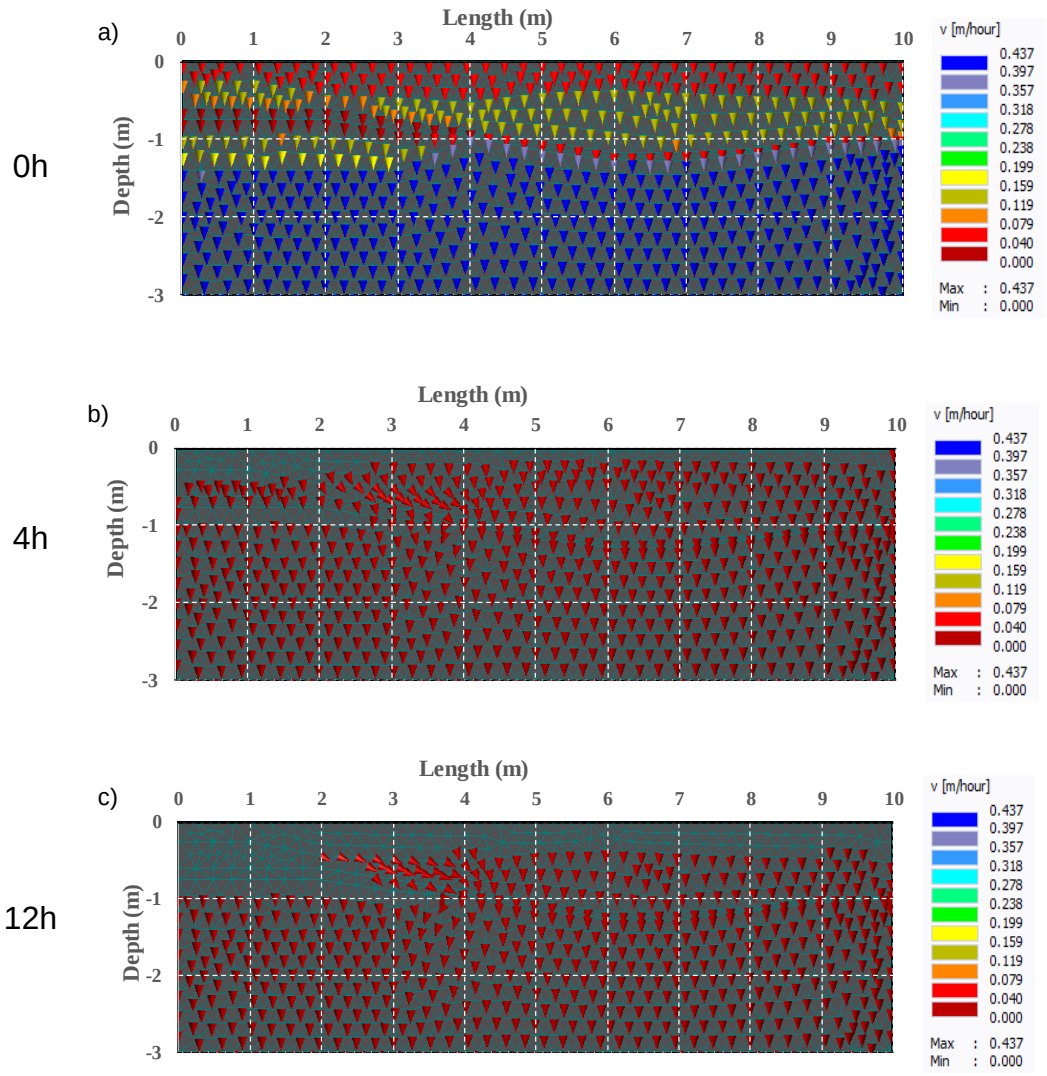

4. Conclusion

The infiltration tests showed the heterogeneity influence on water flow, where the cumulative infiltration presents a big difference between them. Furthermore, the linearization presented a decrease in the gravitational influence, where on the contact line of the different layers it causes a reduction in the hydraulic conductivity.

The Hydrus simulation demonstrated a high influence of the soil heterogeneity in the water flow. This is due to the differences between the soil hydrodynamic properties and the existing materials in the available profile. The profile textural heterogeneity generated the appearance of a preferential flow.

The GPR mapping showed 4 different geological units on the profile. Thus, it could be observed that even with certain interpretation limitations, the methodology helped to identify the different lithofacies. However, the existing soil type could not be determined, requiring a local sample for this characterization. Nevertheless, when

the GPR technique is used in conjunction with other forms of soil physical characterization, it becomes a tool with a good level of precision.

5. References

Aiello, R., Bangarelo, V., Barbagallo, S., Consoli, S., Di Prima, S., Giordano, G., Iovino, M. (2014) An assessment of the Beerkan method for determining the hydraulic properties of a sandy loam soil. Geoderma, v. 235–236, p. 300–307.

Alagna, V., Bangarelo, V., Di Prima, S., Giordano, G., Iovino, M. (2016) Testing infiltration run effects on the estimated water transmission properties of a sandy-loam soil. Geoderma, v. 267, p. 24-33.

Antonino, A. C. D., Ângulo-Jaramillo, R., Souza, E. S., Netto, A. M., Carneiro, C. J. G. & Montenegro, A. A. A. (2001) Determinação da condutividade hidráulica e Determinação da condutividade hidráulica e da sorvidade de um solo com infiltrômetro a disco. Revista Brasileira de Engenharia Agrícola e Ambiental, v.5, n.2, p.247-253, Campina Grande, PB.

Araújo Filho, P. F., Cabral, J. J. da S. P., Braga, R. A. P. (2015) Importância da camada de solo no leito de rios intermitentes na proteção do aquífero: estudo de caso. 12º SISLUBA.

Arya, L.M., Paris, J. F. A. (1981) Physicoempirical model to predict soil moisture characteristics from particle-size distribution and bulk density data. Soil Sci. Soc. Am. J. 45:1023–1030. ISBN 978-85-61428-23-5.

Braga, R. A. P. (2016) Águas invisíveis nos rios intermitentes. Cap. 1, 11p, 1 in: Águas de Areias, Recife. 336p.

Coutinho, A., Lassabatere, L., Winiarski, T., Cabral, J., Antonino, A. and Angulo-Jaramillo, R. (2015) Vadose Zone Heterogeneity Effect on Unsaturated Water Flow Modeling at Meso-Scale. Journal of Water Resource and Protection, 7, 353-368. doi: 10.4236/jwarp.2015.74028.

Brooks and Corey (1964) Hydraulic properties of porous media. Hydrology papers University Fort Collins.

Burdine N. T. (1953). Relative permeability calculations from pore size distribution data. Journal of Petroleum Technology 5 (03): 71–78.

Cirilo, J. A., Montenegro, S. M. G. L., Campos, J. N. B. (2017) The Issue of Water in the Brazilian Semi-Arid Region. Book: Waters of Brazilians. pp 59-71. DOI. 10.1007/978-3-319-41372-3_5.

CPRM. (2005) Projeto cadastro de fontes de abastecimento por água subterrânea – Estado de Pernambuco. Ministério de Minas e Energias.

Di Prima, S., Lassabatere, L., Bagarello,V., Iovino, M., Angulo-Jaramillo, R. (2016) Testing a new automated single ring infiltrometer for Beerkan infiltration experiments. Geoderma, v. 262, p. 20–34.

EMBRAPA. (2000) Levantamento de reconhecimento de baixa e média intensidade dos solos do estado de Pernambuco.

Fuentes C, Haverkamp R, Parlange J-Y. 1(992) Parameter constraints on closed-form soilwater relationships. Journal of hydrology 134 (1): 117–142.

Goutaland, D.; Winiarski, T.; Dubé, J. S.; Bièvre, G.; Boucristiani, J. F.; Chouteau, M.; Giroux, B. (2008) Hydrostratigraphic characterization of glaciofluvial deposits underlying an infiltration basin using ground penetrating radar. Vadose Zone Journal. Vol. 7. P. 194-207 . 2008.

Haverkamp R, Debionne D, Viallet P, Angulo-Jaramillo R, de Condappa D. (2006) Soil Properties and Moisture Movement in the Unsaturated Zone. In The Handbook of Groundwater Engineering, Delleur JW (ed.). CRC Press: Indiana; 1–59.

Haverkamp, R., Ross, P. J., Smettem, K. R. J., Parlange, J. Y. (1994) Three-dimensional analysis of infiltration from the disc infiltrometer. 2. Physically based infiltration equation. Water Resources Research, v. 30, p. 2931-2935.

Lassabatère, L., Angulo-Jaramillo, R., Soria Ugalde, J. M., Cuenca, R., Braud, I., Haverkamp, R. (2006) Beerkan estimation of soil transfer parameters through infiltration experiments: BEST. Soil Sci. Soc. Am. J., v. 70, p. 521–532.

Lassabatere L, Angulo-Jaramillo R, Soria-Ugalde JM, Simunek J, Haverkamp R. (2009) Numerical evaluation of a set of analytical infiltration equations.Water Resources Research 45.

Lèger, E., Saintenoy, A, Coquet, Y. (2013) Hydrodynamic parameters of a sandy soil determined by ground-penetrating radar inside a single ring infiltrometer. Water Resour. Res., 50, 5459–5474, doi:10.1002/ 2013WR014226.

MIALL, A. D. (1981) Analysis of fluvial depositional systems. Tulsa: University of Toronto.

Nasta, P., Lassabaterè, L., Kandelous, M. M., Simunek, J., Angulo-Jaramilo, R. (2012) Analysis of the role of tortuosity and infiltration constants in the beerkan method. SSSAJ. Vol. 76. P.1999-2005.

Neal, A. Ground-penetrating radar and its use in sedimentology: principles, problems and progress. Earth-Science Reviews. Vol 66. P. 261-330. 2004.

Prédélus, D., Coutinho, A. P., Lassabatere, L., Bien, L. B., Winiarski, T., Angulo-Jaramillo, R. (2015) Combined effect of capillary barrier and layered slope on water, solute and nanoparticle transfer in an unsaturated soil at lysimeter scale. Journal of Contaminant Hydrology, v. 181 p. 69–81.

Ribeiro Filho, J. C., Palácio, H. A. de Q., Andrade, E. M., Santos, J. C. N., Brasil, J. B. (2017) Rainfall characterization and sedimentological responses of watersheds

with different land uses to precipitation in the semiarid region of Brazil. Rev. Caatinga, Mossoró, v. 30, n. 2, p. 468 – 478, abr. – jun. ISSN 1983-2125 (online).

Smettem, K. R. J., Parlange, J. Y., Ross, P. J. and Haverkamp, R. (1994) Three-dimensional analysis of infiltration from the disc infiltrometer,1, Theoretical capillary approach Water Resour Res.,30, 2925-2929.

van Genuchten, M. Th. (1980) A Closed-form Equation for Predicting the Hydraulic Conductivity of Unsaturated Soils.

Vandervaere, J.-P., Vauclin, M., Elrick, D.E. (2000) Transient flow from tension infiltrometers: I. The two-parameter equation. Soil Science Society of American Journal, Vol. 64, p. 1263-1272.

Winiarski, T., Lassabatère, L., Ângulo-Jaramillo, R., Goutaland, D. (2013) Characterization of the heterogeneous flow and pollutant transfer in the unsaturated zone in the fluvio-glacial deposit. Procedia Environmental Sciences, v. 19, p. 955-964. Agricultural Water Management 176, 243–254.

Xi, B., Bloomberg, M., Watt, M. S., Wang, Y. Jia, L. (2016) Modeling growth response to soil water availability simulated by HYDRUS for a mature triploid Populus tomentosa plantation located on the North China Plain.